

図5  
合成高分子の例

起こる重合は薬物キャリアの用途には使えない」のではなく、目的とする高分子の分子量、分子量分布、化学的純度、重合後の精製の容易さ、製造コストなどの諸要素を勘案したうえで、高分子の種類および重合法の選定を行うことが重要なことを述べたいのである。

以下に、薬物キャリアとして用いられている合成高分子3種について、構造と合成について簡単に解説する。

### ビニル系高分子

ビニル系高分子とは、図5aに示すような二重結合を有するモノマーが重合したものである。その主鎖はポリエチレンと同じもので、生体内非分解性である。この系統の高分子を応用した薬物キャリアで有名な2例は、スマンクス<sup>11,12)</sup>と後述するPHPMA<sup>7,13)</sup>である。いずれも一般的なラジカル重合で得られる高分子なので、目的を達成するための重合条件や精製法を検討したうえで用いている。

### ポリアミノ酸

図5bに示すポリアミノ酸は比較的研究の歴史は古く、1980年代からポリ(グルタミン酸)<sup>14,15)</sup>などが研究されてきた。最近の臨床例では、抗がん剤パクリタキセルを結合したポリ(グルタミン酸)がphase IIIの検討まで進んだのが有名である<sup>16)</sup>。筆者らの高分子ミセルの研究・開発例でも一つの高分子鎖としてポリ(アスパラギン酸)を中心に検討が進められて

きた<sup>17)</sup>。

ポリアミノ酸は比較的副反応が少なく、狭い分子量分布が得られる高分子で、この特長もこの用途に使用されてきた有力な要因の一つである。

### ポリエチレングリコール

上記の2例と異なり、ポリエチレングリコール(PEG)は、高分子の分類名ではなく単一の高分子鎖である。すでにインターフェロンなどの生理活性蛋白質の修飾で実用化されている。また、リボソームの表面修飾剤や高分子ミセルの外殻構成成分として使われている。この高分子は図5cに示すように、エチレンオキシドをアニオン重合という方法で得るが、副反応はほとんどなく、鎖状の高分子構造のみが得られる。また、高分子の末端構造の制御が容易で、狙った官能基を末端に効率高く導入が可能である。

PEGは生体中で不活性である特徴とともに、この末端構造制御が容易であることが、薬物キャリア研究に数多く用いられている大きな要因である。たとえば、蛋白をPEGで化学修飾する場合、PEG鎖1本当たり一つの末端の反応性官能基数が理想である。これが少ないと修飾効率が低くなるし、逆にこの数が1より多い(たとえば両末端にある)と望ましくない架橋構造を形成してしまう。一般に、高分子の末端化学構造の定量的な制御は難しいのであるが、PEGの場合には比較的制御が容易である特長がある。

## 高分子キャリアの設計概念

高分子キャリアの設計概念とされるものが四つ知られてきた。この四つを早く出現した順番に簡単に紹介したい。

### 1. 魔法の弾丸

19世紀末に Paul Ehrlich によって提唱された“魔法の弾丸”は、最初の薬物ターゲティングのアイデアである。特定の種類の細胞にのみ選択的に結合する物質を選択的薬剤として用いるというアイデアである。このアイデアの一つの延長線上に、選択的に結合する物質をキャリアとして用いるのが薬物キャリアへの応用となる。

この“魔法の弾丸”が提示する概念は、現在では古典的なものとなったが、その本質はいささかも重要性を失ってはいない。この概念は現在でも、アクティブターゲティングの主要ななすものである。

### 2. Lysosomotropic agent (1973年)

de Duve は、細胞中のリソゾームに選択的に取り込まれて薬効を発揮するシステムを考案した<sup>18)</sup>。このアイデアは、リソゾームの消化酵素機能や低いpHなどを利用して細胞内の薬物デリバリーに活用しようというものである。エンドサイトーシスされると、消化酵素を含んだリソゾームと融合して二次リソゾームとなる。よって、薬物ターゲティングでは、細胞内に薬物を送達させて薬効を発揮しようとする高分子キャリアシステムにおいて、その多くの場合にエンドサイトーシスを経ることになるので、lysosomotropic agent の概念は重要といえるのである。de Duve は、この概念のDNAをキャリアにした抗がん剤のデリバリーシステムも開発していた<sup>6)</sup>。

### 3. Ringsdorf の高分子医薬モデル (1975年)

Ringsdorf は、1975年に図6に示す高分子をキャリアとしたターゲティングシステムの設計論を提示した<sup>19)</sup>。このモデル提唱以前は、“魔法の弾丸”での薬物とキャリアの二つの要素による設計論であったが、高分子医薬モデルでは五つの要素に増えている。このシステムは、polymer backbone, transport

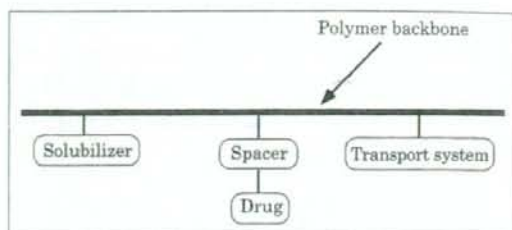


図6 Ringsdorf の高分子医薬のモデル

system, spacer, drug, そして solubilizer からなっている。

Transport system とは、“魔法の弾丸”でのキャリアに相当するものである。Polymer backbone は、“魔法の弾丸”にくらべると新たに加わった要素で、他の要素を結合する土台が用意されることで、工学的なキャリアシステムの設計が可能となる。薬物(drug)は spacer を介して、あるいは介さないで polymer backbone に結合する。Solubilizer とは、疎水性薬物が多く結合してシステムが水に溶けにくくなった場合に、その水溶性を改善する役割を担うものと、その逆に細胞との相互作用を増加させるために疎水性を与える役割を担う二つの場合がある。前者の水溶性 solubilizer の部分をブロックコポリマーの1成分で与えることによって、高分子を会合させるという高分子ミセルキャリアのアイデアに結びつく。Ringsdorf は、1984年に最初の高分子ミセル薬物キャリアの論文を発表している<sup>20)</sup>。

このRingsdorfモデルの提唱は、薬物ターゲティングシステムの工学的な設計論を提示した点で、歴史的にも重要であり、提唱からすでに四半世紀を過ぎている現在でもなお、このモデルは一つのスタンダードとして活用されている。

### 4. EPR 効果 (1986年)

1986年、前田、松村によって発見された高分子物質一般が固形がんを選択的に集積し、保持されるという性質で、固形がん組織へのパッシブターゲティングが高分子や微粒子キャリア一般で可能となる<sup>11,12,21)</sup>。ここで重要なことは、この選択的な高分子物質の集積には特別な高分子(特異抗体など)である必要がないことである。この理論の発見により、固形がんへの passive targeting の研究・開発が飛

躍的に進むことになった一方、抗体をキャリアとしたシステムにおいても、がん組織への集積は passive な機構によることが理解されることで、この active targeting に対しても大きな貢献をしたといえる。

## 高分子キャリアの例

### 1. 水溶性ビニル系高分子キャリア

Kopecek (アメリカ, Utah 大学) と Duncan (イギリス, Carfdiff 大学) は、ポリ(2-ヒドロキシプロピル)メタクリルアミド (PHPMA) を用いたシステムを開発した<sup>7,13)</sup>。これは水溶性のビニル系の合成高分子である PHPMA を主鎖とし、四つのアミノ酸よりなるオリゴペプチドスパーサーを介して薬物をつなげることにより、血液中では安定で標的細胞に取り込まれたのち、リソゾーム酵素によってこのオリゴペプチドスパーサーが開裂して薬物を放出するシステムを実現した。これは、上記で述べた de Duve の lysosomotropic agent と Ringsdorf の高分子医薬のモデルを実現させたものである。

薬物として抗がん剤アドリアマイシンを用い、PK1 と名付けられた最初の passive な固形がんターゲットシステムはイギリスで臨床試験が行われたが、認可には至らなかった。このうち、active な要素を加えた PK2 などでのさらなる臨床試験を目指している。

この PHPMA に抗がん剤のアドリアマイシンを結合させたシステムの設計上の特徴は薬物導入量と分子量にある。アドリアマイシンの結合量を 8wt.% というかなり小さい値に抑えて、ポリマーによる EPR 効果に基づいた固形がん組織へのターゲティング能をアドリアマイシンの疎水性が妨害しないようにしている。また、この高分子は生体内非分解性であるため、その分子量を 3 万未満に抑えて、腎臓からの排出を確保している。

### 2. デキストラン

デキストランは、生体に対して不活性で無毒(あるいはきわめて低活性・低毒性)であると考えられる多糖で、蛋白質の場合に大きな問題となりうる異

種蛋白の抗原性・病原性ウイルスの混入の危険が少ないと考えられ、薬物や造影剤のキャリアとして多用されている天然高分子である。

ここで紹介したいのは、デキストランに正荷電、負荷電の修飾を行って体内での動態を測定した橋田、高倉らの研究<sup>3)</sup>である。電気的に中性のデキストランに少量の負荷電修飾することで肝臓での取り込み、腎臓での排出ともに低下する。一方、正荷電修飾の場合には逆に両者ともに増加する。

以上の結果は、少量の化学修飾による物性の変化(この場合は荷電の変化)が、高分子の体内動態を大きく変化させることを示したことに大きな意義がある。

### 3. 高分子ミセルキャリア

高分子ミセル型ドラッグキャリアシステムは、二つの異なる高分子鎖が直列につながったブロックコポリマーからミセル構造を形成させるものである<sup>17,22,23)</sup>。ブロックコポリマーで用いられているのは、ポリエチレングリコール(PEG)とポリアミノ酸からなるもの、PEG とポリエステル系高分子からなるもの、PEG とビニル系高分子からなるものがある。これらの高分子に共通していることは、以下の事項である。

いずれも分子量分布が狭く、副反応が起こりにくい重合法によって得られたものを用いている。高分子ミセル形成挙動は、各成分のホモポリマー(1種類のモノマーだけからなる高分子)が不純物として混じることと、分子量分布によって大きな影響を受けるからである。よって薬物キャリアとしての性能を再現性よく確保するためには、分子量分布が狭く、ホモポリマーの混在のないブロックコポリマーが用いられるのである。一般に、ビニル系高分子やポリエステル系高分子は、分子量分布の広いものが多いが、高分子ミセルに用いられる場合は、狭い分子量分布が得られる高分子の種類と重合法が慎重に選択されている。

いずれも PEG 鎖がミセル外殻形成高分子鎖として用いられている。この理由は二つある。一つは、PEG が生体内での不活性な性質を利用するためである。二つ目の理由は、PEG 鎖自身の分子量分布

が狭く、副反応がほとんどなく得られる高分子であるとともに、もう一方の高分子鎖を狭い分子量分布で副反応を少なく得るための重合基点としてすぐれているからである。

非水溶性の高分子鎖を用いることのデメリットが少ない。高分子ミセルキャリアは短期的(数時間～数日)には数十nmの粒子として血流中に存在するので、腎臓からの速やかな排泄を免れうる。一方、長期的には高分子鎖1本ずつに解離しうるので、用いるブロックコポリマーの分子量を3万程度以下に抑えておけば、非生体内分解性の高分子を用いることが可能である。

## おわりに

通常、学会や論文発表では「～の高分子を用いて、～の結果を得た」というのみで、なぜその高分子が選ばれたかの高分子化学上の理由を説明することはまれである。また、この理由は高分子の領域以外の方々には、推定しにくいものである。

本稿では、この高分子化学的理由の面になるべく焦点を当てて解説した。しかし、紙面上では書ききれなかった箇所も多くあった。それらは、今後のDDS学会大会や、本誌の特集などで補われることを、筆者は願っている。

## 文 献

- 1) Ayame H, Morimoto N, Akiyoshi K: Self-assembled cationic nanogels for intracellular protein delivery. *Bioconjug Chem* 19: 882-890, 2008.
- 2) Shimizu T, Kishida T, Hasegawa U, Ueda Y, Imanishi J, Akiyoshi K et al.: Nanogel DDS enables sustained release of IL-12 for tumor immunotherapy. *Biochem Biophys Res Commun* 367: 330-335, 2008.
- 3) Takakura Y, Hashida M: Macromolecular carrier systems for targeted drug delivery: pharmacokinetic considerations on biodistribution. *Pharm Res* 13: 820-831, 1996.
- 4) Hardwicke J, Ferguson EL, Moseley R, Stephens P, Thomas DW, Duncan R: Dextrin-rhEGF conjugates as bioresponsive nanomedicines for wound repair. *J Control Release* 130: 275-283, 2008.
- 5) Hreczuk-Hirst D, Chicco D, German L, Duncan R: Dextrins as potential carriers for drug targeting: tailored rates of dextrin degradation by introduction of pendant groups. *Int J Pharm* 230: 57-66, 2001.
- 6) Trouet A, Campeneere DDD, de Duve C: Chemotherapy through lysosomes with a DNA-daunorubicin complex. *Nature New Biol* 239: 110-112, 1972.
- 7) Seymour LW, Miyamoto Y, Maeda H, Strohalm J, Ulbrich K, Duncan R et al.: Influence of molecular weight on passive tumour accumulation of a soluble macromolecular drug carrier. *Eur J Cancer* 31A: 766-770, 1995.
- 8) Svenson S, Tomalia DA: Dendrimers in biomedical applications-reflections on the field. *Adv Drug Deliv Rev* 57: 2106-2129, 2005.
- 9) 鶴田禎二, 川上雄資: 高分子設計. 日刊工業新聞社, 1996.
- 10) 井上祥平: 高分子合成化学. 裳華房, 1996.
- 11) 前田 浩: Polymer drugsのその後と今後 Overview-スマンクスからEPR効果へ-. *Drug Delivery Systems* 16: 136-142, 2001.
- 12) Maeda H: The enhanced permeability and retention (EPR) effect in tumor vasculature: the key role of tumor-sective macromolecular drug targeting. *Adv Enzyme Regul* 41: 189-207, 2001.
- 13) Putnam D, Kopecek J: Polymer conjugates with anticancer activity. *Advances in Polymer Science* 122: 55-123, 1995.
- 14) Nukui M, Hoes K, van den Berg H, Feijen J: Association of macromolecular prodrugs consisting of adriamycin bound to poly (L-glutamic acid). *Makromol Chem* 192: 2925-2942, 1991.
- 15) Tsukada Y, Kato Y, Umemoto N, Takeda Y, Hara T, Hirai H: An anti- $\alpha$ -fetoprotein antibody-daunorubicin conjugate with a novel poly-L-glutamic acid derivative as intermediate drug carrier. *J Natl Cancer Inst* 73: 721-729, 1984.
- 16) Singer JW: Paclitaxel poliglumex (XYOTAX, CT-2103): a macromolecular taxane. *J Control Release* 109: 120-126, 2005.
- 17) Yokoyama M: Polymeric micelles for the targeting of hydrophobic drugs. (ed. Kwon GS). *Drug and Pharmaceutical Sciences vol.148: Polymeric Drug Delivery Systems*. Taylor & Francis, Boca Raton, FL, USA, 2005, p533-575.
- 18) de Duve CE, de Barsey T, Poole B, Trouet A, Tulkens P, van Hoof F: Commentary: Lysosomotropic agent. *Biochem Pharmacol* 23: 2495-2531, 1973.
- 19) Ringsdorf H: Structure and properties of pharmacologically active polymers. *J Polymer Sci Symposium* 51: 135-153, 1975.
- 20) Bader H, Ringsdorf H, Schmidt B: Watersoluble polymers in medicine. *Angew Chem* 123/124: 457-485, 1984.
- 21) Matsumura Y, Maeda M: A new concept for macromolecular therapeutics in cancer chemotherapy: Mechanism of tumorotropic accumulation of proteins and the antitumor agent smancs. *Cancer Res* 46: 6387-6392, 1986.
- 22) Aliabadi HM, Lavasanifar A: Polymeric micelles for drug delivery. *Expert Opin Drug Deliv* 3: 139-162, 2006.
- 23) 横山昌幸: 高分子ミセルターゲティング. 炎症と免疫 16: 21-26, 2008.



## Efficient peritoneal dissemination treatment obtained by an immunostimulatory phosphorothioate-type CpG DNA/cationic liposome complex in mice

Yukari Kuramoto, Shigeru Kawakami, Shuwen Zhou, Kyouichi Fukuda, Fumiyo Yamashita, Mitsuru Hashida\*

*Departments of Drug Delivery Research, Graduate School of Pharmaceutical Sciences, Kyoto University, Sakyo-ku, Kyoto 606-8501, Japan*

Received 27 September 2007; accepted 7 December 2007

Available online 31 January 2008

### Abstract

Peritoneal dissemination remains the most difficult type of metastasis to treat, and current systemic chemotherapy or radiotherapy tends to have little effect; therefore, immunotherapy using immunostimulatory CpG DNA could be a promising new therapeutic approach. Recently, we have reported that intraperitoneal administration of phosphodiester (PO) CpG DNA-lipoplex could efficiently inhibit peritoneal dissemination in mice. In this study, chemically modified phosphorothioate (PS)-CpG DNA and natural PO-CpG DNA were complexed with DOTMA/cholesterol cationic liposomes (PS-CpG DNA-lipoplex and PO-CpG DNA-lipoplex) and their antitumor activity was evaluated in a mouse model of peritoneal dissemination. Intraperitoneal administration of the PS-CpG DNA-lipoplex inhibited the proliferation of tumor cells in the greater omentum and the mesentery more efficiently than PO-CpG DNA-lipoplex. PS-CpG DNA-lipoplex induced higher cytokine production from primary cultured mouse peritoneal macrophages, suggesting that the high antitumor activity of the PS-CpG DNA-lipoplex is mediated by a high rate of cytokine production from immunocompetent cells such as macrophages. The serum transaminase levels of mice receiving intraperitoneal PS-CpG DNA-lipoplex treatment were measured to evaluate systemic toxicity, and these were found to be the same as those of untreated mice. These results suggest that intraperitoneal administration of PS-CpG DNA-lipoplex could be efficient immunotherapy for peritoneal dissemination. © 2008 Elsevier B.V. All rights reserved.

**Keywords:** CpG DNA; Phosphorothioate; Peritoneal dissemination; Cationic liposome; Macrophage

### 1. Introduction

Peritoneal dissemination remains the most difficult type of metastasis to treat, and current systemic chemotherapy or radiotherapy tends to have little effect. The therapeutic problem of peritoneal dissemination is trans-lymphatic metastasis, that is, migration of the peritoneal free cancer cells through the lymphatic tissue, such as the milky spot on the greater omentum, spreading metastases throughout the body [1]. Since there are many immunocompetent cells in the lymphatic tissue, activation of these cells would be a new therapeutic strategy for peritoneal dissemination. It has been reported that CpG DNA,

about 30-base oligonucleotides containing CpG dinucleotides, which is derived from the bacterial DNA, is recognized by Toll-like receptors (TLR)-9 expressed by macrophages and dendritic cells and induces Th1 type antitumor cytokines, such as tumor necrosis factor (TNF)- $\alpha$  and interleukin (IL)-12 [2,3]. Therefore, delivery of CpG DNA into lymphatic immunocompetent cells via the peritoneal cavity and induction of Th1 type cytokines in lymphatic tissues would effectively inhibit peritoneal dissemination.

As far as the molecular weight of the intraperitoneally injected compounds is concerned, a value of over 50,000 is required for efficient lymphatic organ distribution [4]. Since the molecular weight of naked CpG DNA is about 8000, intraperitoneally administered naked CpG DNA cannot reach lymphatic organs. In fact, Agrawal et al. have reported that

\* Corresponding author. Tel.: +81 75 753 4525; fax: +81 75 753 4575.  
E-mail address: [hashidam@pharm.kyoto-u.ac.jp](mailto:hashidam@pharm.kyoto-u.ac.jp) (M. Hashida).

intraperitoneally administered 20 mer naked oligonucleotide distributed into the blood and distributed in the kidney as well as intravenously administered oligonucleotide [5]. Since liposome-entrapped compounds are selectively distributed to the lymphatic organs following intraperitoneal administration [6,7], CpG DNA/cationic liposomes complex (lipoplex) formation is expected to enhance the distribution of CpG DNA to lymphatic organs. Recently, we have reported that intraperitoneal administration of phosphodiester (PO) CpG DNA-lipoplexes ranging in size from 100 to 200 nm could efficiently inhibit peritoneal dissemination in a mouse model [8].

In this study, we found that phosphorothioate (PS)-CpG DNA-lipoplex produced better therapeutic effects on peritoneal dissemination than PO-CpG DNA-lipoplex in mice. As far as the mechanism of the antitumor activity of the PS-CpG DNA-lipoplex was concerned, we also found that PS-CpG DNA-lipoplex resulted in significantly higher cytokine production than PO-CpG DNA-lipoplex after being taken up by macrophages. PS-CpG DNA-lipoplex or PO-CpG DNA-lipoplex were administered intraperitoneally using a peritoneal dissemination model in mice which involved the intraperitoneal inoculation of colon26/Luc cells, a mouse colorectal adenocarcinoma cell line that stably expresses firefly luciferase gene. We previously reported that some tumor cells are present in the lymphatic system (greater omentum) 24 h after intraperitoneal inoculation of tumor cells [9]. Therefore, in order to ensure the adhesion and invasion of the tumor cells in the lymphatic organs, PS-CpG DNA-lipoplex was administered 3 days after tumor cell inoculation. The numbers of tumor cells were quantitatively evaluated by measuring the luciferase activity in the greater omentum and the mesentery as the index of peritoneal dissemination [10,11]. In addition, TNF- $\alpha$  contributes to the antitumor activity and, therefore, the TNF- $\alpha$  produced by immunocompetent cells in response to TLR-9 activation was measured using the primary cultured mouse peritoneal macrophages.

## 2. Materials and methods

### 2.1. Animals

Male Balb/c (6-week-old) mice and female ICR (4-week-old) mice were purchased from the Shizuoka Agricultural Cooperative Association for Laboratory Animals (Shizuoka, Japan). Animals were maintained under conventional housing conditions. All animal experiments were approved by the Animal Experimentation Committee of the Graduate School of Pharmaceutical Sciences, Kyoto University.

### 2.2. Chemicals

RPMI1640 medium, phosphate buffered saline (PBS), Hanks' balanced salt solution (HBSS), and TGC medium were obtained from Nissui Pharmaceutical Co., Ltd. (Tokyo, Japan). Opti-MEM I was obtained from Invitrogen (Carlsbad, CA). Fetal bovine serum (FBS) was obtained from MP Biomedicals, Inc. (Irvine, CA). *N*-[1-(2,3-dioleoyloxy)propyl]-

*N,N,N*-trimethylammonium chloride (DOTMA) was purchased from Tokyo Chemical Industry, Co., Ltd. (Tokyo, Japan) and cholesterol was from Nacalai Tesque Inc. (Kyoto, Japan). Oligonucleotides with phosphorothioate and phosphodiester backbones were purchased from Operon (Tokyo, Japan). The sequences of the oligonucleotides were 5'-TCGACGTTTTG-ACGTTTTGACGTTTT-3' (CpG DNA) and 5'-TGACGCTTTGAGCTTTTGTAGCTTTT-3' (control GpC DNA). The level of TNF- $\alpha$  from the culture supernatant was determined by the ELISA Ready-SET-go! set (eBioscience, San Diego, CA). All other chemicals were of the highest grade available.

### 2.3. Preparation of liposomes and their complex with CpG DNA

Cationic liposomes were prepared as reported previously [12]. In brief, DOTMA and cholesterol were mixed in chloroform at a molar ratio of 1:1, then the mixture was dried, vacuum-desiccated, and resuspended in 5% dextrose solution in sterile test-tubes. After hydration for 30 min at room temperature, the dispersion was sonicated for 10 min in a bath sonicator, then for 3 min in a tip sonicator to form liposomes and, finally, sterilized by passing through a 0.45- $\mu$ m filter (Nihon-Millipore Ltd., Tokyo, Japan). Liposome/CpG DNA complexes were prepared as described in previous reports [8]. An equal volume of stock liposome solution and CpG DNA in 5% dextrose were mixed at various charge ratios, and left at 37 °C for 30 min. The mean particle size and  $\zeta$ -potential of the lipoplexes were measured using a Zetasizer nano ZS instrument (Malvern Instruments, UK).

### 2.4. Cell lines

Murine adenocarcinoma colon 26 tumor cells [13] was grown in 5% CO<sub>2</sub> in humidified air at 37 °C with RPMI1640 medium supplemented with 10% FBS, 100 IU/ml penicillin, 100  $\mu$ g/ml streptomycin, and 2 mM L-glutamine. Colon26 cells that stably express the firefly luciferase gene (colon26/Luc) were established as previously reported [14,15].

### 2.5. Peritoneal dissemination model and the antitumor activity of the CpG DNA-lipoplex

Colon26/Luc cells were trypsinized, and the cell concentration was adjusted to 10<sup>6</sup> cells/ml in HBSS. Then, 0.1 ml of the cell suspension was inoculated intraperitoneally into male Balb/c mice. Three days after tumor inoculation, 5% dextrose, naked PS- and PO-CpG DNA (1  $\mu$ g/mouse), PS- and PO-CpG DNA-lipoplex (1  $\mu$ g/mouse at the charge ratio 3.1) were administered to the peritoneal cavity of mice (0.2 ml 5% dextrose solution/mouse). Ten days after tumor inoculation, the mice were euthanized by cervical dislocation and the greater omentum and mesentery were excised and washed with ice-cold saline. Then, the organs were homogenized in a lysis buffer (0.05% Triton X-100, 2 mmol/l EDTA, 0.1 mol/l Tris pH 7.8), and centrifuged at 10,000 g for 10 min. Ten microliter of the supernatant was mixed with 100  $\mu$ l luciferase assay buffer (Picagene, Toyo Ink,

Tokyo Japan), and the light produced was measured in a luminometer (Lumat LB 9507, EG & G Berthold, Bad Wildbad, Germany). The luciferase activity of the peritoneal organs was converted to the number of colon26/Luc cells using a regression line as previously reported [8,15].

### 2.6. *In vitro* cytokine production from primary cultured peritoneal macrophages

Peritoneal macrophages from mice were cultured according to our previous report [16]. Briefly, peritoneal macrophages were obtained from ICR mice 6 days after intraperitoneal injection of 1 ml 3% thioglycollate medium. Collected macrophages were plated on 24-well culture plates at a density of  $1 \times 10^6$  cells/ml and cultured for 24 h. Cells were washed with 0.5 ml PBS before use. The cells were incubated with Opti-MEM containing PS-CpG DNA-lipoplex, PO-CpG DNA-lipoplex, or PS-GpC DNA-lipoplex (5  $\mu$ g DNA/ml) for 2 h, then, washed with PBS and incubated with Opti-MEM. Six or twenty-four after incubation, the supernatants were collected and ELISA used to determine TNF- $\alpha$ .

### 2.7. Evaluation of ALT and AST in serum after intraperitoneal administration of PS-CpG DNA-lipoplex

PS-CpG DNA-lipoplex (1  $\mu$ g/mouse, charge ratio 3.1) was intraperitoneally administered to ICR mice. Blood was collected from the vena cava at 6, 24, and 48 h and allowed to coagulate for 8 h at 4 °C then serum was isolated as the supernatant fraction following centrifugation at 2000 g for 10 min. Serum ALT and AST were measured by the transaminase C II test Wako kit.

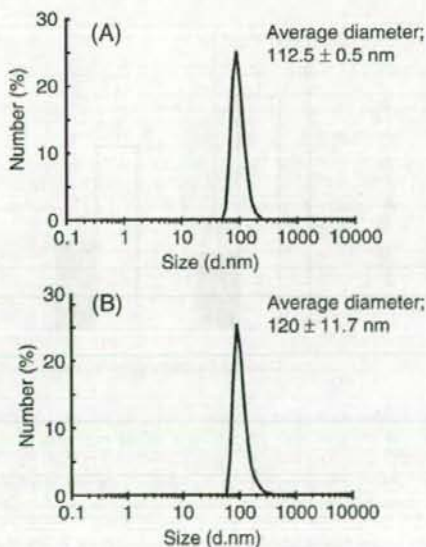


Fig. 1. Particle size distribution of (A) PS-CpG DNA-lipoplex and (B) PO-CpG DNA-lipoplex.

### 2.8. Statistical analysis

Statistical comparisons were performed by Student's *t*-test for two groups and one-way ANOVA for multiple groups. Post hoc multiple comparisons were made using Tukey's test.  $P < 0.05$  was considered significant.

## 3. Results

### 3.1. Particle size and $\zeta$ -potential of the PS-CpG DNA-lipoplex and PO-CpG DNA-lipoplex

To investigate the physicochemical properties of the PS-CpG DNA-lipoplex and PO-CpG DNA-lipoplex, their particle sizes and  $\zeta$ -potential were determined. Both lipoplexes showed a clear-cut distribution pattern, and the mean particle size of the PS-CpG DNA-lipoplex (A) and the PO-CpG DNA-lipoplex (B) were  $112.5 \pm 0.5$  nm and  $120 \pm 11.7$  nm, respectively (Fig. 1).  $\zeta$ -potential analysis showed that the  $\zeta$ -potential of the PS-CpG DNA-lipoplex and the PO-CpG DNA-lipoplex were  $53 \pm 0.2$  mV and  $52 \pm 0.3$  mV, respectively ( $n=3$ ). These results showed that there were no differences in terms of particle size and electric charge of the two lipoplexes.

### 3.2. Inhibition of peritoneal dissemination by intraperitoneal administration of PS-CpG DNA-lipoplex

The antitumor effects of the intraperitoneally administered PS-CpG DNA-lipoplex and the PO-CpG DNA-lipoplex on peritoneal dissemination were analyzed. Fig. 2 shows the number of tumor cells in the greater omentum (A) and the mesentery (B) after intraperitoneal administration of PS-CpG DNA-lipoplex and PO-CpG DNA-lipoplex at a DNA dose of 1  $\mu$ g/mouse. In the PS-CpG DNA-lipoplex-treated group, the number of tumor cells in the greater omentum was about 9% compared with that of the PO-CpG DNA-lipoplex-treated group. The number of tumor cells in the mesentery of the PS-CpG DNA-lipoplex-treated mice was about 2% compared with that of the PO-CpG DNA-lipoplex-treated group. The number of tumor cells in the greater omentum (A) and the mesentery (B) after intraperitoneal administration at the DNA dose of 10  $\mu$ g/mouse was also shown in Fig. 3. Intraperitoneal administration of PS-CpG DNA-lipoplex could reduce the numbers of tumor cells in both organs, and the number of tumor cells in the mesentery of the PS-CpG DNA-lipoplex-treated mice was significantly lower than that of PO-CpG DNA-lipoplex-treated mice.

### 3.3. Induction of TNF- $\alpha$ from primary cultured mouse peritoneal macrophages after treatment with PS-CpG DNA-lipoplex

As a mechanism of the antitumor activity of the PS-CpG DNA-lipoplex, the immunostimulatory effect of the PS-CpG DNA-lipoplex was evaluated using primary cultured mouse peritoneal macrophages. Primary cultured mouse peritoneal macrophages were treated with PS-CpG DNA-lipoplex and produced a higher level of TNF- $\alpha$  in the culture medium than

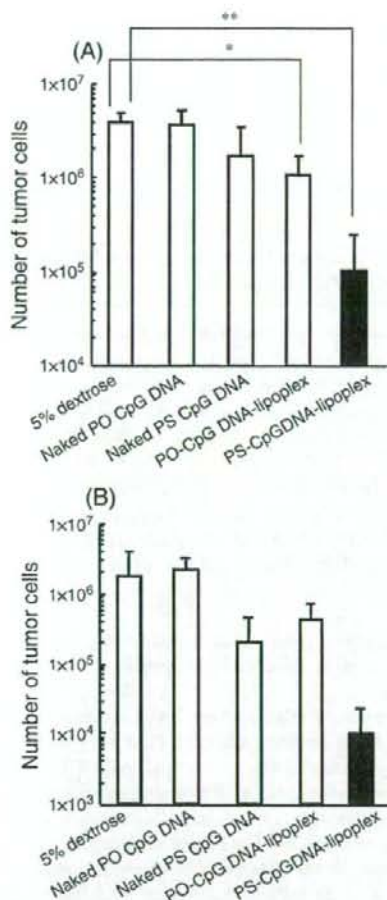


Fig. 2. The number of tumor cells in the (A) greater omentum and (B) mesentery of the peritoneal dissemination mice after intraperitoneal administration of PS-CpG DNA-lipoplex and PO-CpG DNA-lipoplex. Balb/c mice were intraperitoneally administered 5% dextrose, naked PS-CpG DNA, naked PO-CpG DNA, PS-CpG DNA-lipoplex and PO-CpG DNA-lipoplex after an intraperitoneal inoculation of colon26/Luc cells. Ten days after tumor inoculation, the luciferase activity of the greater omentum and the mesentery was measured and converted into the number of tumor cells. Results are expressed as mean+SD ( $n=4$ ). \* $P<0.05$ , \*\* $P<0.01$ ; The number of tumor cells was significantly different from 5% dextrose-treated group.

those treated with PO-CpG DNA-lipoplex (\*\* $P<0.001$ ). On the other hand, PS-CpG DNA-lipoplex, which had no CpG motifs, did not induce any TNF- $\alpha$  production.

### 3.4. Evaluation of ALT and AST in serum after intraperitoneal administration of PS-CpG DNA-lipoplex

To evaluate the intraperitoneal administration of PS-CpG DNA-lipoplex, serum ALT and AST levels were measured. The ALT and AST levels in the serum of PS-CpG DNA-lipoplex-treated mice were the same as those of untreated mice (Fig. 5).

## 4. Discussion

To date, there are many reports about refractory peritoneal dissemination therapy using particle formation of chemotherapeutic agents with a low molecular weight based on enhancement of distribution in the lymphatic organs [4,17,18]. However, chemotherapy causes severe side-effects, therefore, immunotherapy would be a more promising approach.

The therapeutic problem associated with peritoneal dissemination is trans-lymphatic metastasis. As shown in Fig. 1, the particle size of both CpG DNA-lipoplexes was about 100 nm. These results suggest that both CpG DNA-lipoplexes could be more efficiently distributed to lymphatic organs than naked CpG DNA. In peritoneal dissemination model, PS-CpG DNA-lipoplex inhibited the proliferation of tumor cells more effectively compared with PO-CpG DNA-lipoplex after intraperitoneal administration (Figs. 2 and 3). High antitumor effects of

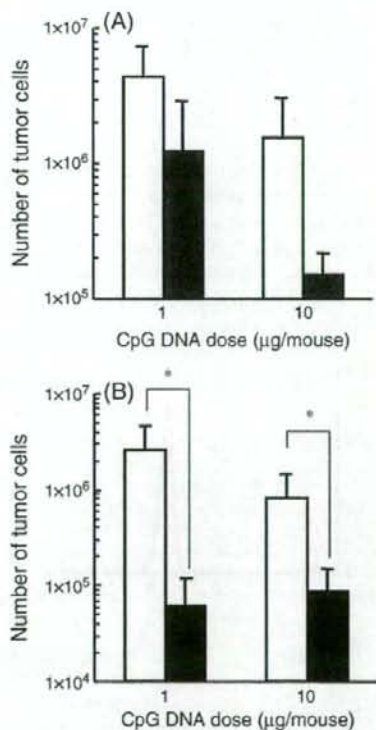


Fig. 3. Dose-dependent effect of intraperitoneally administered PS-CpG DNA-lipoplex and PO-CpG DNA-lipoplex in a mouse peritoneal dissemination model. Balb/c mice were intraperitoneally administered PS-CpG DNA-lipoplex (■) and PO-CpG DNA-lipoplex (□) at a dose of 1  $\mu$ g or 10  $\mu$ g DNA/mouse after an intraperitoneal inoculation of colon26/Luc cells. Ten days after tumor inoculation, the luciferase activity of the greater omentum (A) and the mesentery (B) was measured and converted into the number of tumor cells. Results are expressed as mean+SD ( $n=4$ ). \* $P<0.05$ ; The number of tumor cells of PS-CpG DNA-lipoplex-treated group was significantly different from PO-CpG DNA-lipoplex-treated group.



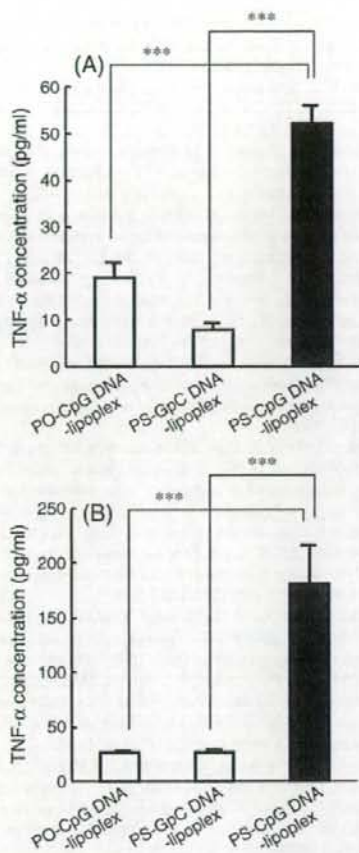


Fig. 4. TNF- $\alpha$  production from primary cultured mouse peritoneal macrophages after treatment with PS-CpG DNA-lipoplex. Primary cultured mouse peritoneal macrophages were treated with PS-CpG DNA-lipoplex, PO-CpG DNA-lipoplex, and PS-GpC DNA-lipoplex (no CpG motifs). The concentration of TNF- $\alpha$  in the culture medium after 6 h (A) and 24 h (B) incubation was determined by ELISA. Results are expressed as mean  $\pm$  SD ( $n=3$ ). \*\*\* $P<0.001$ ; The TNF- $\alpha$  concentration of PS-CpG DNA-lipoplex treatment group was significantly different from PO-CpG DNA-lipoplex and PS-GpC DNA-lipoplex treatment group.

PS-CpG DNA-lipoplex might be mediated by the high immunostimulatory effect of PS-CpG DNA-lipoplex; therefore, TNF- $\alpha$  production was measured as an index of immunostimulation, using primary cultured mouse peritoneal macrophages. TNF- $\alpha$  production from PS-CpG DNA-lipoplex-treated cells was significantly higher than that from PO-CpG DNA-lipoplex (Fig. 4). Taking these findings consideration, the high antitumor effect of the PS-CpG DNA-lipoplex might be due to the potent immunostimulatory activity of the PS-CpG DNA-lipoplex after being taken up by immunostimulatory cells.

As far as the application of naked CpG DNA is concerned, PS modification has been widely used for protection from nuclease degradation. It has been found that peritumoral administration of naked PS-CpG DNA eradicated tumor growth

by local induction of NK cells and CD8<sup>+</sup> T cells in solid tumor-bearing mice [19]. Another group have shown that intradermal administration of naked PS-CpG DNA around the tumor inhibits tumor growth and metastasis of melanoma cells [20]. In this study, naked PS-CpG DNA-lipoplex and PO-CpG DNA-lipoplex were intraperitoneally administered to treat peritoneal dissemination. However, as shown in Fig. 2, not only naked PO-CpG DNA but also naked PS-CpG DNA failed to inhibit the proliferation of tumor cells in the mouse peritoneal dissemination model. This lack of inhibition might be explained by the fact that the molecular weight of both naked CpG DNAs is about 8000, which is not high enough to distribute to the lymph organs after intraperitoneal administration [4].

For clinical application of intraperitoneal PS-CpG DNA-lipoplex, not only the efficacy but also the toxicity has to be considered. To date, there are many reports about the toxicity of systemic administration of plasmid DNA/cationic liposome complex (pDNA-lipoplex). Loisel S. et al. have reported that the main toxicity of systemically administered pDNA-lipoplex is observed in the liver and not the lung [21]. In this study, PS-CpG DNA-lipoplex was given intraperitoneally, however, if any intraperitoneally administered PS-CpG DNA-lipoplex was absorbed into the bloodstream, it might cause systemic toxicity. Therefore, the hepatic toxicity of intraperitoneally injected PS-CpG DNA-lipoplex was evaluated. As shown in Fig. 5, the serum ALT and AST levels of mice treated with PS-CpG DNA-

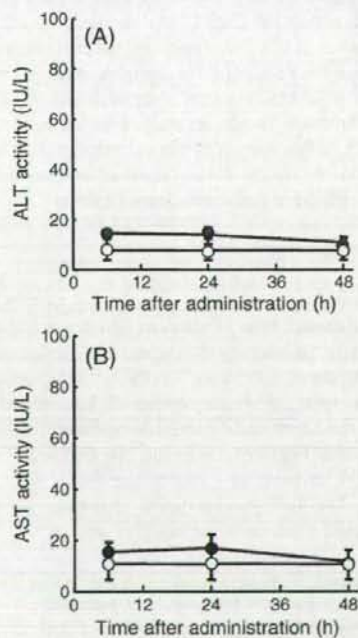


Fig. 5. Evaluation of hepatic toxicity after intraperitoneal administration of PS-CpG DNA-lipoplex. PS-CpG DNA-lipoplex (●) was administered to ICR mice. (○) represents the no treatment group. Serum ALT (A) and AST (B) levels 6, 24, and 48 h after administration were measured. Results are expressed as mean  $\pm$  SD ( $n=4$ ).

lipoplex (1  $\mu\text{g}$  DNA/mouse) were the same as those of untreated mice after intraperitoneal administration, suggesting that no hepatic toxicity was induced. These results for the hepatic toxicity correspond to an earlier report that the serum ALT level after intraperitoneal administration of pDNA-lipoplex (15  $\mu\text{g}$  DNA/mouse) was within the normal range [22].

Recently, Edelstein et al. described the use of gene therapy in clinical trials [23]. According to the review, lipoplexes have already been used as a non-viral delivery vector. As far as the evaluation of the side effects of intraperitoneally administered lipoplex in clinical situations is concerned, Mudhusudan et al., have reported that no severe toxicity was observed at a DNA dose of 1.8 mg/m<sup>2</sup>, and this DNA dose is equal to the dose of 15  $\mu\text{g}$ /mouse [24]. In this study, we have demonstrated the potential use of PS-CpG DNA-lipoplex for therapeutic effects against peritoneal dissemination even at a DNA dose as low as 1  $\mu\text{g}$ /mouse. Taking these findings into consideration, safe and effective peritoneal dissemination therapy using PS-CpG DNA-lipoplex could be used in clinical applications in the future.

It was also reported that CpG DNA reversed the immunosuppression state caused by chemotherapeutic agent [25,26]; therefore, combination of PS-CpG DNA-lipoplex and chemotherapy is expected to enhance the therapeutic effect against peritoneal dissemination by reversing the immunosuppressed state.

In conclusion, we have demonstrated that PS-CpG DNA-lipoplex exhibits more potent therapeutic effects on peritoneal dissemination than PO-CpG DNA-lipoplex after intraperitoneal administration in mice. A suggested mechanism for the anti-tumor activity of PS-CpG DNA-lipoplex is the higher cytokine production from macrophages compared with PO-CpG DNA-lipoplex. Although further investigations are needed to clarify the efficacy of this system in clinical practice, this information will be valuable for the development of immunotherapy treatments for refractory peritoneal dissemination.

#### Acknowledgements

This work was supported in part by Grants-in-Aid for Scientific Research from Ministry of Education, Culture, Sports, Science, and Technology of Japan, by Health and Labour Sciences Research Grants for Research on Advanced Medical Technology from the Ministry of Health, Labour and Welfare of Japan, by the Mochida Memorial Foundation for Medical and Pharmaceutical Research and by the 21st Century COE Program "Knowledge Information Infrastructure for Genome Science".

#### References

- Y. Yonemura, Y. Endo, T. Obata, T. Sasaki, Recent advances in the treatment of peritoneal dissemination of gastrointestinal cancers by nucleoside antimetabolites, *Cancer Sci.* 98 (1) (2007) 11–18.
- A.M. Krieg, A.-K. Yi, S. Matson, T.J. Waldschmidt, G.A. Bishop, R. Teasdale, G.A. Koretzky, D.M. Klinman, CpG motifs in bacterial DNA trigger direct B-cell activation, *Nature* 374 (6522) (1995) 546–549.
- H. Hemmi, O. Takeuchi, T. Kawal, T. Kaisho, S. Sato, H. Sanjo, M. Matsumoto, K. Hoshino, H. Wagner, K. Takeda, S. Akira, A toll-like receptor recognizes bacterial DNA, *Nature* 408 (6820) (2000) 740–745.
- K. Hirano, C.A. Hunt, Lymphatic transport of liposome-encapsulated agents: effects of liposome size following intraperitoneal administration, *J. Pharm. Sci.* 74 (9) (1985) 915–921.
- S. Agrawal, J. Tamsamani, T.Y. Tang, Pharmacokinetics, biodistribution, and stability of oligodeoxynucleotide phosphorothioates in mice, *Proc. Natl. Acad. Sci. USA* 88 (1991) 7595–7599.
- R.J. Perker, K.D. Hertman, S.M. Sleber, Lymphatic absorption and tissue disposition of liposome-entrapped [<sup>14</sup>C] adriamycin following intraperitoneal administration to rats, *Cancer Res.* 41 (4) (1981) 1311–1317.
- W.T. Phillips, L.A. Medina, R. Klipper, B. Goins, A novel approach for the increased delivery of pharmaceutical agents to peritoneum and associated lymph nodes, *J. Pharmacol. Exp. Ther.* 303 (1) (2002) 11–16.
- Y. Kuramoto, M. Nishikawa, K. Hyoudou, F. Yamashita, M. Hashida, Inhibition of peritoneal dissemination of tumor cells by single dosing of phosphodiester CpG oligonucleotide/cationic liposome complex, *J. Control. Release* 115 (2) (2006) 226–233.
- K. Hyoudou, M. Nishikawa, Y. Kobayashi, Y. Kuramoto, F. Yamashita, M. Hashida, Inhibition of adhesion and proliferation of peritoneally disseminated tumor cells by pegylated catalase, *Clin. Exp. Metastasis* 23 (5–6) (2006) 269–278.
- Y. Ikehara, T. Niwa, L. Biao, S.K. Ikehara, N. Ohashi, T. Kobayashi, Y. Shimizu, N. Kojima, H. Nakanishi, A carbohydrate recognition-based drug delivery and controlled release system using intraperitoneal macrophages as a cellular vehicle, *Cancer Res.* 66 (17) (2006) 8740–8748.
- M.J. Lee, S.S. Cho, J.R. You, Y. Lee, B.D. Kang, J.S. Choi, J.W. Park, Y.L. Suh, J.A. Kim, D.K. Kim, J.S. Park, Intraperitoneal gene delivery mediated by a novel cationic liposome in a peritoneal disseminated ovarian cancer model, *Gene Ther.* 9 (13) (2002) 859–866.
- S. Kawakami, A. Sato, M. Nishikawa, F. Yamashita, M. Hashida, Mannose receptor-mediated gene transfer into macrophages using novel mannose-ligated cationic liposomes, *Gene Ther.* 7 (4) (2000) 292–299.
- T.H. Corbett, D.P. Griswold Jr., B.J. Roberts, J.C. Peckham, F.M. Schabel Jr., Tumor induction relationships in development of transplantable cancers of the colon in mice for chemotherapy assays, with a note on carcinogen structure, *Cancer Res.* 35 (1975) 2434–2439.
- K. Hyoudou, M. Nishikawa, Y. Uneyama, Y. Kobayashi, F. Yamashita, M. Hashida, Inhibition of metastatic tumor growth in mouse lung by repeated administration of polyethylene glycol-conjugated catalase: quantitative analysis with firefly luciferase-expressing melanoma cells, *Clin. Cancer Res.* 10 (22) (2004) 7685–7691.
- K. Hyoudou, M. Nishikawa, Y. Kobayashi, Y. Kuramoto, F. Yamashita, M. Hashida, Inhibition of adhesion and proliferation of peritoneally disseminated tumor cells by pegylated catalase, *Clin. Exp. Metastasis* 23 (5–6) (2006) 269–278.
- T. Takagi, M. Hashiguchi, R.I. Mahato, H. Tokuda, Y. Takakura, M. Hashida, Involvement of specific mechanism in plasmid DNA uptake by mouse peritoneal macrophages, *Biochem. Biophys. Res. Commun.* 245 (3) (1998) 729–733.
- Y. Sadzuka, S. Hirota, T. Sonobe, Intraperitoneal administration of doxorubicin encapsulating liposomes against peritoneal dissemination, *Toxicol. Lett.* 116 (2000) 51–59.
- C.L. Zavaleta, W.T. Phillips, A. Soundararajan, B.A. Goins, Use of avidin/biotin-liposome system for enhanced peritoneal drug delivery in an ovarian cancer model, *Int. J. Pharm.* 337 (1–2) (2007) 316–328.
- Y. Kawarada, R. Ganss, N. Garbi, T. Sacher, B. Arnold, G.J. Hammerling, NK- and CD8<sup>+</sup> T cell-mediated eradication of established tumors by peritoneal injection of CpG-containing oligodeoxynucleotides, *J. Immunol.* 167 (9) (2001) 5247–5253.
- N. Kuninaka, K. Sano, M. Honda, I. Kuniaki, J. Matsunaga, R. Okuyama, K. Takahashi, H. Watanabe, G. Tamura, H. Tagami, T. Terui, Peritoneal CpG oligodeoxynucleotide treatment inhibits tumor growth and metastasis of B16F10 melanoma cells, *J. Invest. Dermatol.* 123 (2) (2004) 395–402.
- S. Loisel, C.L. Gall, L. Doucet, C. Ferec, V. Flock, Contribution on plasmid DNA to hepatotoxicity after systemic administration of lipoplexes, *Hum. Gene Ther.* 12 (6) (2001) 685–696.
- X. Xing, L. Liu, W. Xia, L.C. Stephens, L. Huang, G. Lopez-Berestein, M.-C. Hung, Safety studies of the intraperitoneal injection of E1A-liposome complex in mice, *Gene Ther.* 4 (3) (1997) 238–243.

## NOTE

# Mannosylated Cationic Liposomes/CpG DNA Complex for the Treatment of Hepatic Metastasis after Intravenous Administration in Mice

YUKARI KURAMOTO, SHIGERU KAWAKAMI, SHUWEN ZHOU, KYOICHI FUKUDA, FUMIYOSHI YAMASHITA, MITSURU HASHIDA

Department of Drug Delivery Research, Graduate School of Pharmaceutical Sciences, Kyoto University, Sakyo-ku, Kyoto 606-8501, Japan

Received 19 November 2007; accepted 19 May 2008

Published online 11 July 2008 in Wiley InterScience (www.interscience.wiley.com). DOI 10.1002/jps.21475

**ABSTRACT:** Immunotherapy using immunostimulatory CpG DNA could be a promising new therapeutic approach to combat refractory hepatic metastasis. In this study, we report the use of a conventional cationic liposomes/CpG DNA complex (Bare/CpG DNA lipoplex) and a mannosylated cationic liposomes/CpG DNA complex (Man/CpG DNA lipoplex) for effective inhibition of hepatic metastasis in mice. After intravenous administration of Bare/CpG DNA lipoplex, higher amounts of IL-12 and IFN- $\gamma$  were produced in serum or liver compared with naked CpG DNA, and their production was increased further by Man/CpG DNA lipoplex. Then, Bare/CpG DNA lipoplex and Man/CpG DNA lipoplex were administered intravenously to hepatic metastasis model mice, and the numbers of tumor cells (colon26/Luc) were quantitatively assayed. The number of tumor cells in Man/CpG DNA lipoplex-treated mice was same as those in Bare/CpG DNA lipoplex-treated mice. These results suggest that intravenous administration of not only Bare/CpG DNA lipoplex but also Man/CpG DNA lipoplex could be an efficient immunotherapy for hepatic metastasis. © 2008 Wiley-Liss, Inc. and the American Pharmacists Association *J Pharm Sci* 98:1193–1197, 2009

**Keywords:** cancer; gene delivery; gene therapy; liposomes; non-viral gene delivery

## INTRODUCTION

Hepatic metastasis is a common event in the course of gastrointestinal malignancies. Although postoperative therapy is needed for hepatic metastasis, conventional chemotherapy has not proven effective in improving long-term results.<sup>1</sup> CpG DNA, about 30-base oligonucleotides containing

CpG dinucleotides, which is derived from the bacterial DNA, is recognized by Toll-like receptors (TLR)-9 expressed by macrophages.<sup>2</sup> Macrophages treated with CpG DNA induce Th1 type antitumor cytokines, such as interleukin (IL)-12, which, in turn, stimulate the production of interferon (IFN)- $\gamma$  by natural killer cells.<sup>3</sup> There are many resident macrophages, Kupffer cells, in the liver; therefore, delivery of CpG DNA into Kupffer cells and induction of Th1 type cytokines would effectively inhibit hepatic metastasis. However, little naked CpG DNA is thought to distribute in the liver Kupffer cells after intravenous administration, since the molecular weight of naked CpG DNA is about 8,000.

Correspondence to: Mitsuru Hashida (Telephone: +81-75-753-4525; Fax: +81-75-753-4575; E-mail: hashidam@pharm.kyoto-u.ac.jp)

*Journal of Pharmaceutical Sciences*, Vol. 98, 1193–1197 (2009)  
© 2008 Wiley-Liss, Inc. and the American Pharmacists Association

As for the Kupffer cell-selective delivery of oligonucleotide, receptor-mediated uptake is a promising approach because these cells express high levels of mannose receptors.<sup>4</sup> Recently, we developed Man-liposomes that are efficiently taken up by macrophages via mannose receptor-mediated endocytosis. We have also developed a Kupffer cell-specific nuclear factor (NF)- $\kappa$ B decoy transfer system by Man-liposomes.<sup>5</sup> These observations prompted us to investigate whether targeted Kupffer cell delivery could be achieved by a Man-liposomes/CpG DNA complex (Man/CpG DNA lipoplex). This is our initial report of Man/CpG DNA lipoplex for the systemic delivery of CpG DNA for treatment of hepatic metastasis. Naked CpG DNA and a conventional cationic liposomes/CpG DNA complex (Bare/CpG DNA lipoplex) were used as controls.

## MATERIALS AND METHODS

### Animals

Male Balb/c (6-week-old) mice and female ICR (4-week-old) mice were purchased from the Shizuoka Agricultural Cooperative Association for Laboratory Animals (Shizuoka, Japan). All the animals were housed with free access to food and water. The light (dark/light cycle was 2/12 h), temperature, and humidity were constantly maintained throughout the experiments. All animal experiments were approved by the Animal Experimentation Committee of the Graduate School of Pharmaceutical Sciences, Kyoto University.

### Preparation of Liposomes and Their Complex with CpG DNA

Man-liposomes and Bare-liposomes were prepared as reported previously.<sup>6</sup> Stock liposome solutions

and phosphorothioate CpG DNA (5'-TCGACGTTT-GACGTTTTGACGTTTT-3', Operon Biotechnologies, Inc., Tokyo, Japan) in 5% dextrose were mixed at a charge ratio of 1.0:3.1 (-/+), to obtain the Man/CpG DNA lipoplex and the Bare/CpG DNA lipoplex. The mean particle size and  $\zeta$ -potential of the lipoplexes were measured by Zetasizer nano ZS equipment (Malvern Instruments Ltd, Worcestershire, UK).

### Statistical Analysis

Statistical comparisons were performed by one-way ANOVA for multiple groups. Post hoc multiple comparisons were made by using Tukey's test.

## RESULTS AND DISCUSSION

To investigate the physicochemical properties of Man/CpG DNA lipoplex and Bare/CpG DNA lipoplex, their particle sizes and  $\zeta$ -potential were evaluated. The mean particle sizes of the Man/CpG DNA lipoplex and Bare/CpG DNA lipoplex were  $120.0 \pm 1.2$  nm and  $110.6 \pm 0.7$  nm, respectively, and both lipoplexes showed similar and monomodal distribution pattern (Fig. 1). The  $\zeta$ -potential of the Man/CpG DNA lipoplex and the Bare/CpG DNA lipoplex were  $57.8 \pm 0.8$  mV and  $53.0 \pm 0.2$  mV, respectively ( $n = 3$ ).

After intravenous administration of naked CpG DNA, the serum IL-12 concentration was about 200 pg/mL and IFN- $\gamma$  was near the limit of detection at 4 h. These observations of naked CpG DNA agree with the report by Whitmore et al.<sup>7</sup> We previously demonstrated that intravenously administered CpG motif containing plasmid DNA complexed with cationic liposomes composed of DOTMA/cholesterol efficiently pro-

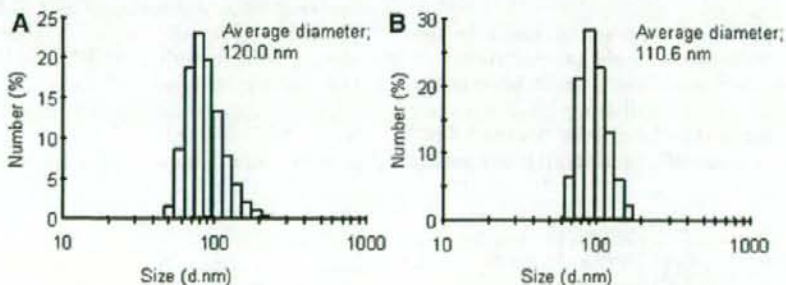


**Figure 1.** Particle size distribution of (A) Man/CpG DNA lipoplex and (B) Bare/CpG DNA lipoplex.

duced IL-12 and IFN- $\gamma$ .<sup>8</sup> Therefore, DOTMA/cholesterol liposomes were selected for delivery of CpG DNA. As shown in Figure 2, when Bare/CpG DNA lipoplex was administered, the levels of IL-12 and, in particular, IFN- $\gamma$  in serum increased compared with naked CpG DNA. Moreover, when Man/CpG DNA lipoplex was administered, the level of both IL-12 and IFN- $\gamma$  in serum was significantly increased compared with Bare/CpG DNA lipoplex (Fig. 2). IL-12 and IFN- $\gamma$  were not detected at 4 h after intravenous administration of unloaded Bare-liposomes (4 mg total lipid/kg) or Man-liposomes (3 mg total lipid/kg). This phenomenon is corresponding to the recent report by Shin et al. that little IFN- $\gamma$  was detected in serum at 6 h after intravenous administration of unloaded cationic liposomes (20 mg total lipid/kg).<sup>9</sup> Similarly, the hepatic concentration of IFN- $\gamma$  was increased by naked CpG DNA, Bare/CpG DNA lipoplex, and Man/CpG DNA lipoplex, in that order (Fig. 3). Previously, we have shown that cultured mouse peritoneal macrophages treated with Bare/GpC DNA-lipoplex, which had no CpG motifs, did not induce any TNF- $\alpha$  production.<sup>10</sup> Taking these into considerations, CpG DNA delivered by Bare- and Man-liposomes could effectively induce the production of Th1 type cytokines in serum and liver after intravenous administration.

The antitumor effects of intravenously administered Bare/CpG DNA lipoplex and Man/CpG DNA lipoplex in the hepatic metastasis model were analyzed using colon26/Luc cells, a murine colorectal adenocarcinoma cell line that stably expresses firefly luciferase gene.<sup>11</sup> The numbers of tumor cells were quantitatively evaluated by measuring the luciferase activity in the liver. As shown in Figure 4, the number of tumor cells in Man/CpG DNA lipoplex- and Bare/CpG DNA lipoplex-treated mice was about 10% compared with that of naked CpG DNA. As far as the antitumor effect of CpG DNA is concerned, Whitmore et al.<sup>7</sup> demonstrated that antitumor effect was correlated with serum Th1 cytokine levels using pulmonary metastasis model. Moreover, Yano et al.<sup>12</sup> also reported that in hepatic metastasis model, intravenously administered cationic liposome/scrambled siRNA complex hardly inhibited the tumor growth in the liver. These observations suggest that cationic liposome/nucleic acid complex did not directly inhibit the hepatic metastasis. The number of tumor cells in naked CpG DNA-treated mice was unexpectedly significantly different from that in

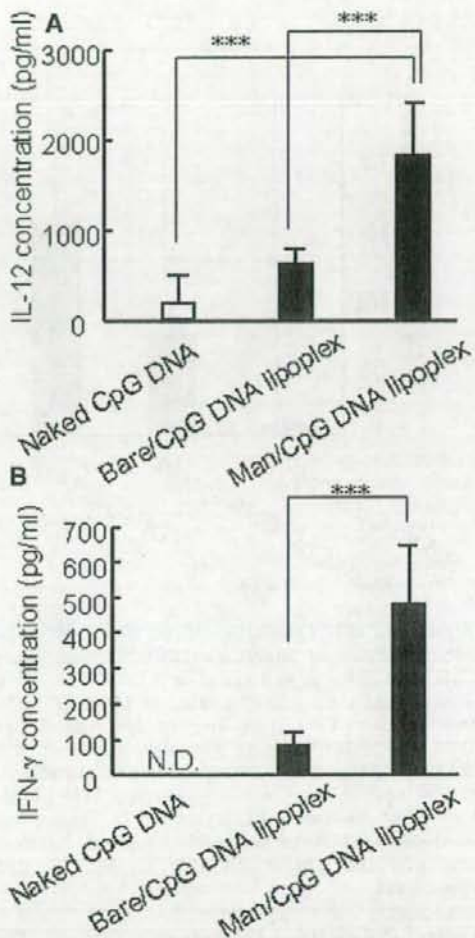


**Figure 2.** IL-12 and IFN- $\gamma$  concentration in serum after intravenous administration of Man/CpG DNA lipoplex, Bare/CpG DNA lipoplex, and naked CpG DNA. The concentrations of IL-12 (A) and IFN- $\gamma$  (B) in serum at 4 h after intravenous administration of Man/CpG DNA lipoplex, Bare/CpG DNA lipoplex, naked CpG DNA (10  $\mu$ g DNA/mouse), were measured by ELISA kits (eBioscience, Inc., San Diego, CA). IL-12 and IFN- $\gamma$  were not detected at 4 h after intravenous administration of unloaded Bare-liposomes (4 mg total lipid/kg) or Man-liposomes (3 mg total lipid/kg; data not shown). The lipid doses of unloaded Bare-liposomes and Man-liposomes were based on the amount of component in a 10  $\mu$ g DNA dose of lipoplex/mouse; thus about 4 mg total lipid/kg for unloaded Bare-liposomes and about 3 mg total lipid/kg for unloaded Man-liposomes were utilized. Results are expressed as mean  $\pm$  SD ( $n \geq 5$ ). \*\*\* $p < 0.001$ ; N.D., not detected.

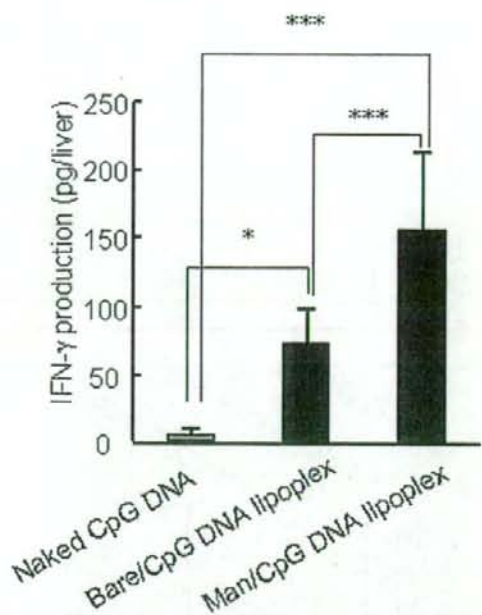


**Figure 3.** IFN- $\gamma$  production in liver after intravenous administration of Man/CpG DNA lipoplex, Bare/CpG DNA lipoplex, and naked CpG DNA. Four hours after intravenous administration of Man/CpG DNA lipoplex, Bare/CpG DNA lipoplex, and naked CpG DNA (10  $\mu$ g DNA/mouse), mice were sacrificed, then the blood in the liver was removed by intraportal injection of 5 mL saline. The concentration of IFN- $\gamma$  in the liver were measured by ELISA kit (R & D Systems, Inc., Minneapolis, MN) as previously described.<sup>15</sup> Results are expressed as mean  $\pm$  SD ( $n = 6$ ). \* $p < 0.05$ ; \*\*\* $p < 0.001$ .

control (5% dextrose-treated) mice (Fig. 4). This result might be supported by the result that naked CpG DNA slightly induced IL-12 in serum (Fig. 2). Taking these into considerations, intravenously administered CpG DNA complexed with Man- and/or Bare-liposomes could effectively inhibit hepatic metastasis with Th1 cytokine production.

Intravenous administration of Bare/CpG DNA lipoplex moderately induced IL-12 and IFN- $\gamma$  production, to inhibit hepatic metastasis as well as Man/CpG DNA lipoplex. These observations about Bare/CpG DNA lipoplex might partly corresponding to our previous report that intravenously administered Bare-liposomes/plasmid DNA complex,<sup>13</sup> and NF- $\kappa$ B decoy oligonucleotides<sup>14</sup> is taken up by the liver non-parenchymal cells mainly via Kupffer cell phagocytosis. Since intravenous administration of Bare-liposomes/

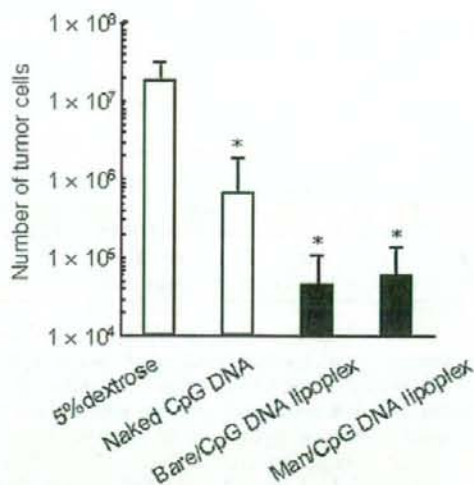


**Figure 4.** The number of tumor cells in the liver of the hepatic metastasis mice after intravenous administration of Man/CpG DNA lipoplex, Bare/CpG DNA lipoplex, and naked CpG DNA. Colon26 cells that stably express the firefly luciferase gene (colon26/Luc)<sup>11</sup> were inoculated intraportally into male Balb/c mice ( $1 \times 10^5$  cells/mouse). Three days later, 5% dextrose, Man/CpG DNA lipoplex, Bare/CpG DNA lipoplex, and naked CpG DNA (10  $\mu$ g DNA/mouse) were administered to the tail vein of the mice. Ten days after tumor inoculation, the luciferase activity of the livers was measured and converted to the number of colon26/Luc cells as previously reported.<sup>10</sup> Results are expressed as mean  $\pm$  SD ( $n \geq 5$ ). \* $p < 0.05$ ; the number of tumor cells was significantly different from 5% dextrose-treated group.

plasmid DNA, which contains CpG motifs, produce IL-12, IFN- $\gamma$ , and TNF- $\alpha$  in serum after taken up by the liver Kupffer cells,<sup>15</sup> Bare-liposomes are an effective carrier to deliver CpG DNA to Kupffer cells.

Immunosuppression is one of the most serious issues raised by systemic chemotherapy using conventional anti-cancer drugs. Recently, it was reported that CpG DNA reversed the reduction in NK cell activity and Th1 type cytokine production by chemotherapeutic agents,<sup>16</sup> and retarded the growth of solid tumors.<sup>17</sup> Therefore, combination of chemotherapy and immunotherapy is expected to enhance the therapeutic effect against hepatic metastasis by reversing the immunosuppressed state. These observations lead us to believe that chemotherapeutic agents and Man/CpG DNA lipoplex will be a promis-

ing combination therapy to combat hepatic metastasis.

In conclusion, intravenously administered Man/CpG DNA lipoplex and/or Bare/CpG DNA lipoplex inhibit hepatic metastasis by the production of IL-12 and IFN- $\gamma$ . Although further investigations are needed to clarify the molecular mechanisms operating in this system, this information will be valuable for the development of immunotherapy to combat refractory hepatic metastasis.

#### ACKNOWLEDGMENTS

This work was supported in part by Grants-in-Aid for Scientific Research from Ministry of Education, Culture, Sports, Science, and Technology of Japan, by Health and Labour Sciences Research Grants for Research on Advanced Medical Technology from the Ministry of Health, Labour and Welfare of Japan, by the Mochida Memorial Foundation for Medical and Pharmaceutical Research, and by the 21st Century COE Program "Knowledge Information Infrastructure for Genome Science."

#### REFERENCES

- Liu XL, Zhang WH, Jiang HC. 2003. Current treatment for liver metastasis from colorectal cancer. *World J Gastroenterol* 9:193-200.
- Krieg AM, Yi AK, Matson S, Waldschmidt TJ, Bishop GA, Teasdale R, Koretzky GA, Klinman DM. 1995. CpG motifs in bacterial DNA trigger direct B-cell activation. *Nature* 374:546-549.
- Chace JH, Hooker NA, Mildenstein KL, Krieg AM, Cowdery JS. 1997. Bacterial DNA-induced NK cell IFN- $\gamma$  production is dependent on macrophage secretion of IL-12. *Clin Immunol Immunopathol* 84:185-193.
- Kuiper J, Brower A, Knook DL, Berkel TJC. 1994. Kupffer and sinusoidal endothelial cells. In: Arias IM, Boyar JL, Fausto N, Jakoby WB, Schachter DA, Shafritz DA, editors. *The liver: biology and pathology*, 3rd edition. New York: Raven Press, Ltd. pp 791-818.
- Higuchi Y, Kawakami S, Oka M, Yabe Y, Yamashita F, Hashida M. 2006. Intravenous administration of mannoseylated cationic liposomes/NF $\kappa$ B decoy complexes effectively prevent LPS-induced cytokine production in a murine liver failure model. *FEBS Lett* 580:3706-3714.
- Kawakami S, Sato A, Nishikawa M, Yamashita F, Hashida M. 2000. Mannose receptor-mediated gene transfer into macrophages using novel mannoseylated cationic liposomes. *Gene Ther* 7:292-299.
- Whitmore MM, Li S, Falo L, Jr., Huang L. 2001. Systemic administration of LPD prepared with CpG oligonucleotides inhibits the growth of established pulmonary metastases by stimulating innate and acquired antitumor immune responses. *Cancer Immunol Immunother* 50:503-514.
- Kawakami S, Ito Y, Charoensit P, Yamashita F, Hashida M. 2006. Evaluation of proinflammatory cytokine production induced by linear and branched polyethylenimine/plasmid DNA complexes in mice. *J Pharmacol Exp Ther* 317:1382-1390.
- Shin D, Kim SI, Park M, Kim M. 2007. Immunostimulatory properties and antiviral activity of modified HBV-specific siRNAs. *Biochem Biophys Res Commun* 364:436-442.
- Kuramoto Y, Kawakami S, Zhou S, Fukuda K, Yamashita F, Hashida M. 2008. Efficient peritoneal dissemination treatment obtained by an immunostimulatory phosphorothioate-type CpG DNA/cationic liposome complex in mice. *J Control Release* 126:274-280.
- Kuramoto Y, Nishikawa M, Hyoudou K, Yamashita F, Hashida M. 2006. Inhibition of peritoneal dissemination of tumor cells by single dosing of phosphodiester CpG oligonucleotide/cationic liposome complex. *J Control Release* 115:226-233.
- Yano J, Hirabayashi K, Nakagawa S, Yamaguchi T, Nogawa M, Kashimori I, Naito H, Kitagawa H, Ishiyama K, Ohgi T, Irimura T. 2004. Antitumor activity of small interfering RNA/cationic liposome complex in mouse models of cancer. *Clin Cancer Res* 10:7721-7726.
- Mahato RI, Kawabata K, Nomura T, Takakura Y, Hashida M. 1995. Physicochemical and pharmacokinetic characteristics of plasmid DNA/cationic liposome complexes. *J Pharm Sci* 84:1267-1271.
- Higuchi Y, Kawakami S, Oka M, Hashida M. 2006. Suppression of TNF $\alpha$  production in LPS induced liver failure in mice after intravenous administration of cationic liposome/NF $\kappa$ B decoy complex. *Pharmazie* 61:144-147.
- Sakurai F, Terada T, Yasuda K, Yamashita F, Takakura Y, Hashida M. 2002. The role of tissue macrophages in the induction of proinflammatory cytokine production following intravenous injection of lipoplexes. *Gene Ther* 9:1120-1126.
- Wang XS, Sheng Z, Ruan YB, Guang Y, Yang ML. 2005. CpG oligodeoxynucleotides inhibit tumor growth and reverse the immunosuppression caused by the therapy with 5-fluorouracil in murine hepatoma. *World J Gastroenterol* 11:220-224.
- Balsari A, Tortoreto M, Besusso D, Petrangolini G, Sfondrini L, Maggi R, Ménard S, Pratesi G. 2004. Combination of a CpG-oligodeoxynucleotide and a topoisomerase I inhibitor in the therapy of human tumour xenografts. *Eur J Cancer* 40:1275-1281.

## Magnetic targeting after femoral artery administration and biocompatibility assessment of superparamagnetic iron oxide nanoparticles

Hui-Li Ma,<sup>1</sup> Xian-Rong Qi,<sup>1</sup> Wu-Xiao Ding,<sup>1</sup> Yoshie Maitani,<sup>2</sup> Tsuneji Nagai<sup>2</sup>

<sup>1</sup>Department of Pharmaceutics, School of Pharmaceutical Sciences, Peking University, Beijing 100083, China

<sup>2</sup>Institute of Medicinal Chemistry, Hoshi University, Shinagawa-Ku, Tokyo 142-850, Japan

Received 14 October 2006; revised 22 December 2006; accepted 30 January 2007

Published online 6 July 2007 in Wiley InterScience (www.interscience.wiley.com). DOI: 10.1002/jbm.a.31346

**Abstract:** Ferrofluids are attractive candidates for magnetic targeting system because of their fluidity and magnetism. The magnetic nanoparticles in ferrofluids should have combined properties of superparamagnetic behavior, target localization, and biocompatibility. The magnetic targeting and biocompatibility of superparamagnetic iron oxide nanoparticles stabilized by alginate (SPION-alginate) was investigated *in vitro* and *in vivo*. The localization of SPION-alginate by an external magnetic field *in vitro* was quantitatively evaluated by determining the iron content, and the results revealed that the localization ratio of SPION-alginate was 56%. Magnetic targeting of the SPION-alginate after femoral artery administration with the magnetic field in rats was quantitatively investigated by iron content and qualitatively confirmed by histological evaluation and magnetic resonance imaging. The ratio of

iron content between the target site and the nontarget site were 8.88 at 0.5 h and 7.50 at 2 h, respectively. The viability of RAW264.7 cells and L929 cells was apparently unaltered upon exposure to SPION-alginate. The incubation with erythrocytes indicated that the SPION-alginate did not induce erythrocytes hemolysis and aggregation. In conclusions, the SPION-alginate had magnetic targeting with an external magnetic field and did not be detained at the injection site without the magnetic field. The SPION-alginate was generally considered to be biocompatible in cytotoxicity and hemolysis aspects. © 2007 Wiley Periodicals, Inc. *J Biomed Mater Res* 84A: 598–606, 2008

**Key words:** superparamagnetic iron oxide nanoparticles (SPION); magnetic targeting; biocompatibility; alginate; localization ratio

### INTRODUCTION

Drug targeting always attracts the most interests from pharmaceutical researchers, among which magnetic drug targeting has been widely studied for the advantages to reduce the amount of drug needed and to reduce the adverse effect of drug. In magnetic targeting, a magnetic compound was injected into the systemic circulation, and then stopped with a powerful magnetic field in the target site.<sup>1</sup> Compared with other targeting vectors, such as ligand-targeting particulates and enzyme-triggered drug release system, magnetic targeting system is feasible to produce, reliable to control and can be specifically

modified for drug delivery applications. Current applications of magnetic targeting system include magnetic delivery of chemotherapy drugs to tumors,<sup>2–4</sup> magnetic targeting of radioisotope,<sup>1,5</sup> magnetic hyperthermia,<sup>6</sup> magnetically enhanced gene therapy,<sup>7</sup> and magnetic embolization.<sup>8</sup> Some successes are achieved, but the results from both laboratory and clinical trials are far from satisfactory. Currently, one of the main problems is that the localization effect of magnetic carrier in target site with the magnetic field is not as good as expected.

Many factors, including physio-chemical properties of magnetic carrier, target sites, magnetic field, and the route of administration, can affect the magnetic targeting effect. When addressing the physio-chemical properties of magnetic carrier, we have to consider the size, magnetization and matrix materials. Magnetic carriers can be grouped into ferrofluids, magnetic nanospheres, and magnetic microspheres according to the size from 10 nm to 100 µm. Ferrofluids are stable colloidal systems that com-

Correspondence to: X.R. Qi; e-mail: qixr2001@yahoo.com.cn  
Contract grant sponsor: National High Technology Research and Development Program of China; contract grant number: 863 Program, No. 2003AA326020



posed of solid, magnetic, single-domain magnetic nanoparticles, typically between 3 and 15 nm in diameter, in a nonmagnetic solvent.<sup>9</sup> Because of the fluidity and magnetism of ferrofluids, they have been widely used in the magnetic targeting system. For biomedical applications, it is required that the magnetic nanoparticles should have combined properties of superparamagnetic behavior, high magnetic saturation, good stability, target localization ability, and biocompatibility. In our laboratory, a kind of ferrofluids, superparamagnetic iron oxide nanoparticles stabilized by alginate (SPION-alginate), was prepared successfully. They were composed of iron oxide ( $\text{Fe}_3\text{O}_4$ ) with 5–10 nm core diameter and had good magnetic susceptibility.<sup>10</sup>

The magnetic field should be of sufficient strength to attract the magnetic particles into the desired area or target site. The higher magnetic flux density and magnetic gradient it is, the better the location effect is.<sup>2</sup> Because of the superparamagnetism and liquid state of ferrofluids, the magnetism of ferrofluids was usually weaker than that of magnetic microsphere. Therefore, a higher magnetic field is needed to attract or hold the injected ferrofluids to the target site.

The route of administration and target site can also greatly affect the magnetic targeting effect. If the target site is a part of reticuloendothelial system (RES), such as liver or spleen, most of magnetic carriers always accumulate in it by the passive targeting effect through intravenous injection. If the target site is a tumor outside RES, the passive accumulation in RES becomes a significant negative factor, and this is one reason why magnetic targeting carrier is still far from satisfactory. Compared with intravenous injection, the artery injection has more advantages, since the magnetic carriers have more chances to access to the target site, avoid clearance by RES, and then stopped by external magnetic field.<sup>2–4</sup>

The term "biocompatibility" encompasses many different properties of the materials, however, two important aspects of the biomaterial screening refer to their *in vitro* cytotoxicity and blood compatibility behavior.<sup>11</sup> The cell lines of mouse fibroblasts (L929) and mouse macrophages (RAW264.7) were widely used in biocompatibility studies. L929 was recommended by many standard institutions as reference cell line for the cytotoxicity testing of polymers<sup>12,13</sup> and RAW264.7 was used for uptake iron oxide nanoparticles.<sup>14</sup>

In this study, we evaluated the magnetic targeting of SPION-alginate with the magnetic field both *in vitro* and *in vivo*. Biocompatibility of SPION-alginate was measured by hemolysis assay and erythrocytes aggregation assay, and *in vitro* cytotoxicity of L929 cells and RAW264.7 cells. Meanwhile, the labeling of RAW264.7 cells with SPION-alginate was examined.

## MATERIALS AND METHODS

### Chemicals and magnetic field

The SPION-alginate was a kind of superparamagnetic iron oxide nanoparticles stabilized by alginate macromolecules with good stability and good magnetism.<sup>10</sup> The SPION-alginate was prepared by a modified two-step coprecipitation method. The ferric and ferrous chlorides (molar ratio of 2:1.5) were dissolved in distilled water and chemical precipitation was achieved by adding 5 mol/L NaOH solution at 60°C. The sodium alginate solution was added to the suspension and was stirred vigorously for 30 min. The mixture was heated at 80°C with slow stirring for 1 h and then sonicated for 20 min. All the above processes were run under total  $\text{N}_2$  protection. The obtained suspension was dialyzed against deionized water. Finally, the suspension was centrifuged at 10,000 rpm for 20 min to remove the solid material, and the black supernatant, namely SPION-alginate, was collected.

The SPION-alginate had a core (iron oxide nanoparticles) diameter of 5–10 nm, a hydrodynamic diameter of 193.8 nm, and  $\zeta$ -potential of  $-67.5$  mV. Saturation magnetization (Ms) of the SPION-alginate in suspension was 40 emu/g at 27°C. T1 relaxivity and T2 relaxivity in 0.9% NaCl solution determined by a 1.5 T MRI scanner at 20°C were  $7.86 \pm 0.20 \text{ s}^{-1} \text{ mM}^{-1}$  and  $281.2 \pm 26.4 \text{ s}^{-1} \text{ mM}^{-1}$ , respectively.<sup>10</sup>

A cuboid permanent neodymium iron boron magnet (NdFeB-permanent magnet) with length, width, and height of 33, 22, and 11 mm, respectively, was purchased from Beijing Sheng Magnetic Science & Tech (Beijing, China). The magnet with the surface magnetic field of 3500 G was used to produce the magnetic field. And all other reagents used were of analytical reagent grade.

### Localization of SPION-alginate with magnetic field *in vitro*

The apparatus of localization of SPION-alginate with external magnetic field *in vitro* was shown in Figure 1. At first, the roller pump was turned on and the rate of distilled water (flow medium) was set to 8 mL/min and 0.5 mL SPION-alginate of 6.04 mg Fe/mL was injected at

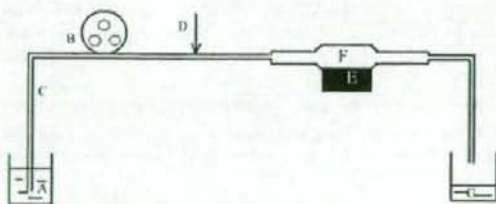


**Figure 1.** The *in vitro* apparatus of location of SPION-alginate with the external magnetic field. (A) flow medium (distilled water, 8 mL/min); (B) roller pump; (C) rubber tube; (D) injection site of SPION-alginate; (E) magnet; (F) glass tube; (G) eluted medium.

the injection part in the rubber tube. At 10 min after circulation, the glass tube with magnet was erected gently to pour the iron oxide particles unlocated tightly. The remnants of SPION-alginate in the glass tube captured by the magnet were separated, and 6M HCl solution was added to dissolve the iron oxide nanoparticles. The iron content was measured by *o*-phenanthroline method.<sup>15</sup> The ratio of iron content captured by the magnet to injected one was referred to as localization ratio *in vitro*. The experiment was repeated in triplicate.

### Magnetic targeting evaluation *in vivo*

Male Sprague-Dawley rats weighing  $250 \pm 20$  g were purchased from Department of Laboratory Animal Science of Peking University Health Science Center. NIH guidelines for the care and use of laboratory animals (NIH Publication #85-23 Rev. 1985) have been observed. Rats were divided into two groups randomly. One group was operated with magnetic field at the right thigh. Before the magnetic targeting of SPION-alginate was carried out, rats were anesthetized by intraperitoneal injection of 1.5 g/kg of ethyl carbamate. The right thigh was disinfected with iodine tincture and 70% alcohol by turns, 30,000 IU penicillin was given by intramuscular injection, and the femoral artery was separated. The SPION-alginate at a dose of 12 mg Fe/kg body weight was injected into the femoral artery at the right thigh under the magnetic field. When the magnetic targeting was performed, the distance between the magnet and the target site was 3 mm, the magnetic field intensity at the target site was 3000 G determined by Gaussmeter, and the magnetic field gradient was 2000 G/cm. The magnetization of SPION-alginate in suspension under the applied magnetic field of 3000 G was 36 emu/g.

After the magnetic targeting, rats were sacrificed by being cut abdominal aorta. The right thigh with magnetic field was referred to as the target site and the left thigh without magnetic field was referred to as the nontarget site in this paper. The right thigh (the target site), left thigh (the nontarget site), liver, and spleen of rats were immediately collected and frozen at  $-20^{\circ}\text{C}$  until analysis. Concerning the thigh of rat, the leg was cut from inguinal groove to knee joint to get thigh part, and the thigh was decorticated, followed by removing the bone, separating the muscle of the thigh. Another group was operated without magnetic field at the right thigh, and other conditions were the same as the group with magnetic field. The iron content in the right thigh, the left thigh, liver, and spleen were determined as follows. The tissues were digested in a beaker with the mixture acid of  $\text{HNO}_3\text{-HClO}_4$  (4:1 v:v) for 48 h at room temperature, and then the solution was evaporated to dryness in sand bath at  $100^{\circ}\text{C}$ . Finally 37.5% HCl was added to the beaker to dissolve the solid and the iron content was determined by *o*-phenanthroline method. The ratio of iron content retained at the right thigh to that of injected was regarded as the localization ratio *in vivo*.

After the magnetic targeting, some of the right thigh (the target site) was intersected, embedded in 4% paraformaldehyde solution (pH 7.4), and then observed at light microscopy after Perls staining and hematoxylin and eosin (H&E) staining.

Ten hours after SPION-alginate application with or without magnetic field on the right thigh, magnetic resonance imaging (MRI) was performed on a 3.0 T clinical MR scanner (GE HD, Milwaukee, WI) with a GPFLEX coil. T2\*-weighted gradient recalled echo (GRE) sequence with a coronary plane was used for imaging with the following parameters: repetition time (TR) of 460 ms; echo time (TE) of 6.6 ms; flip angle of  $25^{\circ}$ ; bandwidth of 62.5 kHz; field of view of  $10 \times 10$  cm, slice thickness of 3 mm with no gap; matrix of  $256 \times 128$ .

### Hemolysis assay *in vitro*

A hemolysis test was performed following the procedure reported previously.<sup>16</sup> The rabbit erythrocyte suspension in 0.9% NaCl (2% (v/v)) was prepared. The SPION-alginate of different concentrations, 0.9% NaCl solution (negative control group as 0% hemolysis) or distilled water (positive control group as 100% hemolysis) was added to the erythrocyte suspension and they were incubated for 3 h at  $37^{\circ}\text{C}$ . After centrifugation at 4000 rpm for 10 min, the absorbance of the supernatant was determined at 540 nm to evaluate the leakage of hemoglobin. Percentage of hemolysis was calculated by  $(A_S - A_N - A_{SB}) / (A_P - A_N) \times 100\%$ , where  $A_S$  was the average absorbance of the SPION-alginate in erythrocyte suspension,  $A_N$  was the average absorbance of 0.9% NaCl solution in erythrocyte suspension (0% hemolysis),  $A_P$  was the average absorbance of distilled water in erythrocyte suspension (100% hemolysis). Because the SPION-alginate still had some extent absorbance at 540 nm after centrifugation, so the average absorbance of SPION-alginate only in 0.9% NaCl solution ( $A_{SB}$ ) is introduced to the equation in order to eliminate the effect of SPION-alginate itself. The experiment was done in triplicate.

### Erythrocytes aggregation assay

Rabbit erythrocytes suspension 200  $\mu\text{L}$  was mixed with the indicated amount of SPION-alginate and incubated for 1 h at  $37^{\circ}\text{C}$  in a 24-well plate. The plate was examined by an inverted microscope (Leica DMIRE2, Germany).

### Cell culture

L929 cells and RAW264.7 cells were cultured in RPMI 1640 medium (Gibco-Invitrogen, NY) supplemented with 10% (v/v) heat-inactivated newborn calf serum (NCS) (Hyclone, USA), 200 U/mL penicillin, 100 U/mL streptomycin, and 0.11 mg/mL sodium pyruvate. Cells were all maintained in a 5%  $\text{CO}_2$  atmosphere at  $37^{\circ}\text{C}$ .

### *In vitro* cytotoxicity evaluation

To determine cytotoxicity, a 3-(4,5-dimethylthiazol-2-yl)-2,5-diphenyl tetrazolium bromide (MTT) assay was performed.<sup>17</sup> The cells were plated at a density of  $5 \times 10^4$  cells/well for RAW264.7 and  $3 \times 10^4$  cells/well for L929 in 96-well plate and cultured for 24 h at  $37^{\circ}\text{C}$  in a 5%  $\text{CO}_2$  atmosphere. For cytotoxicity without NCS, the medium in

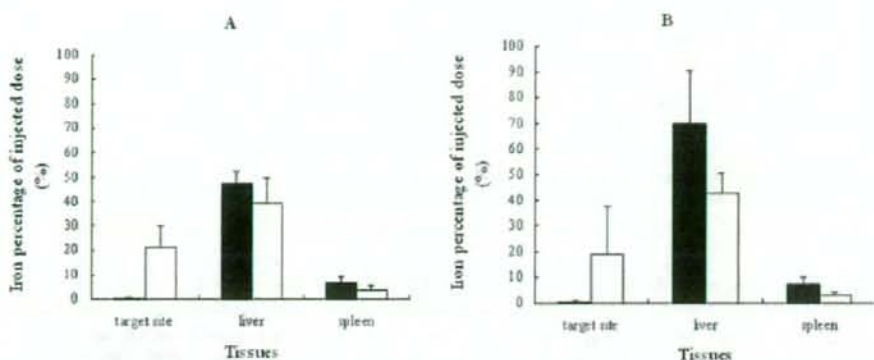


**Figure 2.** The iron percentage of injected SPION-alginate in target site, liver, and spleen with (□) or without (■) 3500 G magnetic field at 0.5 h (A) or 2 h (B) after femoral arterial injection of SPION-alginate at a dose of 12 mg Fe/kg. Data represent mean  $\pm$  SD ( $n = 3$ ).

the wells was replaced with 90  $\mu$ L RPMI 1640 medium, 24 h later, 10  $\mu$ L serial dilutions of the SPION-alginate were added to cells for 24 h with final iron concentrations from 6.25 to 100.0  $\mu$ g/mL, and 10  $\mu$ L RPMI 1640 medium was added to cells as control sample. For cytotoxicity with NCS, the medium in the wells was replaced with 90  $\mu$ L RPMI 1640 medium with 10% NCS and 10  $\mu$ L serial dilutions of SPION-alginate were added with the same iron concentrations as mentioned earlier for 24 h. The cells were washed once with phosphate-buffered saline (PBS, pH 7.4) and replenished with 100  $\mu$ L medium, and then 10  $\mu$ L MTT solution (Sigma, USA) at 5 mg/mL in saline solution was added to each well. After 4 h of incubation, the medium was removed and formazan crystals were solubilized with dimethylsulphoxide (DMSO) for 10 min at room temperature. The absorbance of each well was then measured on a microplate reader (Bio-Rad Model 550, USA) at a wavelength of 570 nm, with 655 nm as a reference wavelength. The relative cell viability (%) related to control wells was calculated by  $(A_{\text{test}}/A_{\text{control}}) \times 100\%$ , where  $A_{\text{test}}$  was the absorbance of the test sample and  $A_{\text{control}}$  was the absorbance of control sample. The experiments were run in hexakis and were repeated three times.

#### Cell labeling with SPION-alginate

RAW264.7 cells were seeded at a density of  $5 \times 10^4$  cells/mL in 35-mm culture plate at 37°C in a 5% CO<sub>2</sub> atmosphere. After 24 h, the SPION-alginate was added to cells with final iron cation concentrations ranging from 12.5 to 50.0  $\mu$ g/mL for various incubation times (1–24 h). And then the cells were washed with PBS to remove excess SPION-alginate. For Prussian blue staining, which indicated the presence of iron, the cells were fixed with 4% glutaraldehyde (Merck, Germany) for 10 min and were washed with PBS, followed by incubation with 2% potassium ferrocyanide in 6% HCl for 30 min. After the wash, they were counterstained with nuclear fast red for 5 min.<sup>18</sup> The specimens were then examined under a light microscope (Olympus BH2, Japan).

## RESULTS

#### Localization of SPION-alginate with magnetic field *in vitro*

From the iron content of SPION-alginate captured by the magnet, the localization ratio *in vitro* was  $(56 \pm 5.1)\%$  ( $n = 3$ ).

#### Magnetic targeting evaluations *in vivo*

Figure 2 showed the iron accumulation in target site, liver and spleen with or without magnetic field via femoral artery injection of SPION-alginate at a dose of 12 mg Fe/kg. At 0.5 h [Fig. 2(A)] and 2 h [Fig. 2(B)] after injection, the localization ratios *in vivo* were about 20%, the iron contents in the right thigh (the target site) with magnetic field were significantly higher than those in the left thigh without magnetic field, and at the same time, the iron contents in liver and spleen with magnetic field were lower than those without magnetic field. The results suggested that the SPION-alginate had some magnetic targeting effect *in vivo*.

In Figure 3, the ratios of iron content (right thigh/left thigh) at 0.5 and 2 h after injection were 1.17 and 1.33 without magnetic field, indicated the SPION-alginate did not be detained in injection site. On the contrary, the ratios of iron content at 0.5 and 2 h after injection were 8.88 and 7.50 with magnetic field, showed the SPION-alginate could be retained at target site with the magnetic field.

With magnetic field at 0.5 h, the femoral artery was filled with iron oxide while the femoral vein was not [Fig. 4(A)], providing a visual evidence for the magnet localization ability of SPION-alginate. Without magnetic field at 0.5 h, the iron oxide was not found

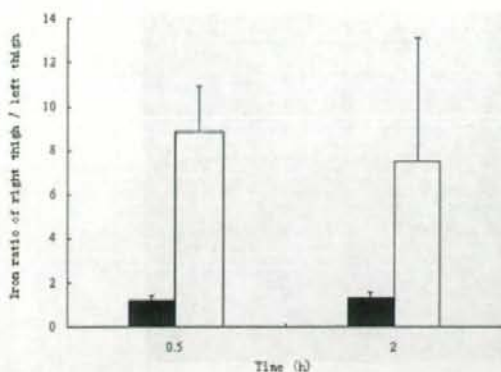


**Figure 3.** Iron ratio of right thigh (target site) and left thigh (nontarget site) with (□) or without (■) magnetic field at 0.5 and 2 h after injection of SPION-alginate. Data represent mean  $\pm$  SD ( $n = 3$ ).

both in femoral artery and in femoral vein [Fig. 4(B)], suggesting that no SPION-alginate was detained in the vascular system without magnetic field.

Iron oxide is well-known to significantly shorten the transverse relaxation times ( $T_2$  or  $T_2^*$ ) with a subsequent loss of MR signal intensity.<sup>19</sup> Therefore,

iron oxide can result in a strong decrease in signal intensity (negative enhancement) of the tissues where they accumulate. Figure 5(A) on  $T_2^*$ -weighted image showed the localization of the iron oxide nanoparticles at the right thigh (circle) with the magnetic field, but no localization was showed without magnetic field [Fig. 5(B)].

#### Hemolysis and erythrocytes aggregation analysis

The leakage of hemoglobin was used to quantify the erythrocytes damage by the SPION-alginate. As shown in Table I, the hemolysis of three preparations of SPION-alginate with different series concentrations were below 5%. So the SPION-alginate did not show hemolytic effect, that is no destruction to the red blood cell membranes. Furthermore, erythrocytes were incubated with the SPION-alginate for 1 h at 37°C, and no aggregation was observed.

#### Cytotoxicity analysis

The results of the MTT assay indicated that the viability of L929 and RAW264.7 apparently unaltered

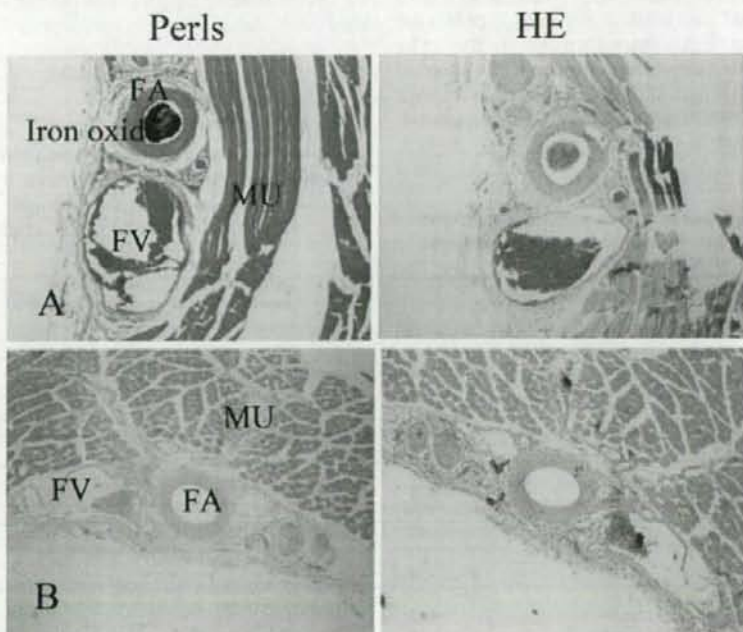


**Figure 4.** Micrographs of rat right thigh (target site) after femoral arterial injection with magnetic field (A) or without magnetic field (B) at 0.5 h. The tissues were stained with H&E and Perls. FA, femoral artery; FV, femoral vein; MU, muscle ( $\times 40$  magnification). [Color figure can be viewed in the online issue, which is available at [www.interscience.wiley.com](http://www.interscience.wiley.com).]